AMERICAN SOCIETY FOR MICROBIOLOGY | Journal of Virology®

CELLULAR RESPONSE TO INFECTION

Suppression of Cytotoxic T Cell Functions and Decreased Levels of Tissue-Resident Memory T Cells during H5N1 Infection

Matheswaran Kandasamy,[a] Kevin Furlong,[a] Jasmine T. Perez,[a] Santhakumar Manicassamy,[b] Balaji Manicassamy[c]

[a]Department of Microbiology, The University of Chicago, Chicago, Illinois, USA
[b]Cancer Immunology, Inflammation, and Tolerance Program, GRU Cancer Center, Augusta University, Augusta, Georgia, USA
[c]Department of Microbiology and Immunology, University of Iowa, Iowa City, Iowa, USA

ABSTRACT Seasonal influenza virus infections cause mild illness in healthy adults, as timely viral clearance is mediated by the functions of cytotoxic T cells. However, avian H5N1 influenza virus infections can result in prolonged and fatal illness across all age groups, which has been attributed to the overt and uncontrolled activation of host immune responses. Here, we investigate how excessive innate immune responses to H5N1 impair subsequent adaptive T cell responses in the lungs. Using recombinant H1N1 and H5N1 strains sharing 6 internal genes, we demonstrate that H5N1 (2:6) infection in mice causes higher stimulation and increased migration of lung dendritic cells to the draining lymph nodes, resulting in greater numbers of virus-specific T cells in the lungs. Despite robust T cell responses in the lungs, H5N1 (2:6)-infected mice showed inefficient and delayed viral clearance compared with H1N1-infected mice. In addition, we observed higher levels of inhibitory signals, including increased PD-1 and interleukin-10 (IL-10) expression by cytotoxic T cells in H5N1 (2:6)-infected mice, suggesting that delayed viral clearance of H5N1 (2:6) was due to the suppression of T cell functions *in vivo*. Importantly, H5N1 (2:6)-infected mice displayed decreased numbers of tissue-resident memory T cells compared with H1N1-infected mice; however, despite the decreased number of tissue-resident memory T cells, H5N1 (2:6) was protected against a heterologous challenge from H3N2 virus (X31). Taken together, our study provides mechanistic insight for the prolonged viral replication and protracted illness observed in H5N1-infected patients.

IMPORTANCE Influenza viruses cause upper respiratory tract infections in humans. In healthy adults, seasonal influenza virus infections result in mild disease. Occasionally, influenza viruses endemic in domestic birds can cause severe and fatal disease even in healthy individuals. In avian influenza virus-infected patients, the host immune system is activated in an uncontrolled manner and is unable to control infection in a timely fashion. In this study, we investigated why the immune system fails to effectively control a modified form of avian influenza virus. Our studies show that T cell functions important for clearing virally infected cells are impaired by higher negative regulatory signals during modified avian influenza virus infection. In addition, memory T cell numbers were decreased in modified avian influenza virus-infected mice. Our studies provide a possible mechanism for the severe and prolonged disease associated with avian influenza virus infections in humans.

KEYWORDS influenza virus, avian H5N1 virus, H1N1 virus, hyperactivation of immune responses, adaptive T cell responses, T cell responses, immune responses

Citation Kandasamy M, Furlong K, Perez JT, Manicassamy S, Manicassamy B. 2020. Suppression of cytotoxic T cell functions and decreased levels of tissue-resident memory T cells during H5N1 infection. J Virol 94:e00057-20. https://doi.org/10.1128/JVI.00057-20.

Editor Tom Gallagher, Loyola University Chicago

Address correspondence to Balaji Manicassamy, balaji-manicassamy@uiowa.edu.

Received 9 January 2020
Accepted 11 February 2020
Accepted manuscript posted online 19 February 2020
Published 16 April 2020

Influenza A viruses, members of the *Orthomyxovirus* family, cause upper respiratory infections in humans (1). Infections by seasonal influenza A virus strains (H1N1 and H3N2) are mostly self-limiting in healthy adults; however, seasonal infections can be severe in young children and the elderly (2, 3). In addition to humans, influenza viruses can infect a variety of zoonotic species, including domestic poultry, pigs, horses, seals, and waterfowl (4–6). Occasionally, influenza virus strains circulating in zoonotic reservoirs can cross the species barrier and cause infections in humans. Unlike seasonal H1N1 and H3N2 strains, infections with avian influenza viruses such as H5N1 and H7N9 are often severe in all age groups and cause extensive alveolar damage, vascular leakage, and increased infiltration of inflammatory cells in the lungs. The virulent nature of avian influenza viruses has been attributed to both viral and host determinants; while the viral determinants of virulence are well defined, the contribution of host responses to disease severity remain to be elucidated.

The H5N1 strain of avian influenza virus was first detected in humans during a domestic poultry outbreak in Hong Kong in 1997 (7, 8). Despite considerable efforts for containment, H5N1 strains have spread globally and are now endemic in domestic poultry on several continents. Over the past 20 years, H5N1 viruses from infected domestic poultry have crossed the species barrier, causing severe and often fatal infections in humans, with mortality rates as high as 60% (9). Many of the viral components critical for the enhanced virulence of H5N1 have been identified through the generation of recombinant and/or reassortant viruses (10–12). Prior studies have shown that the multibasic cleavage site (MBS) in the viral hemagglutinin of H5N1 facilitates higher viral replication and mediates extrapulmonary spread (13–15). In addition, our group has recently demonstrated that the endothelial cell tropism of H5N1 contributes to barrier disruption, microvascular leakage, and subsequent mortality (12). Moreover, polymorphisms that increase viral replication have been identified in the viral polymerase subunits of H5N1 strains (16–20). Together, these studies have helped to define the viral components that are responsible for the enhanced virulence of H5N1.

Apart from viral determinants, overt and uncontrolled activation of the innate immune responses also contribute to the disease severity associated with H5N1 infection (21, 22). Histological analyses of lungs from fatal H5N1 cases demonstrate severe immunopathology, as evidenced by excessive infiltration of immune cells into the lungs and greater numbers of viral antigen-positive cells in the lungs (23, 24). In corroboration with these studies, H5N1 viruses have been shown to induce higher dendritic cell (DC) activation and increase cytokine production compared with H1N1 viruses (25). Moreover, studies with H5N1 strains in animal models demonstrate hyperactivation of resident immune cells in the lungs and a consequent upsurge in cytokine levels (26, 27). As such, these heightened proinflammatory responses result in the excessive recruitment of neutrophils and inflammatory monocytes into the lungs, correlating with severe disease (24). Despite robust activation of innate immune responses against H5N1 infection, higher and prolonged virus replication can be detected in the lungs of infected individuals, suggesting a possible dysregulation of adaptive immune responses (28).

We have previously demonstrated that appropriate activation of respiratory DCs is required for effective T cell responses against a mouse-adapted H1N1 strain (29). Here, we sought to determine if excessive activation of innate immune cells during avian H5N1 infection impairs subsequent adaptive T cell responses. In order to investigate the immune responses against H5N1 compared with a mouse-adapted H1N1 strain, we generated a closely matched recombinant H5N1 virus carrying the 6 internal genes of H1N1 (H5N1 (2:6)). Our studies demonstrated that H5N1 (2:6) infection in mice induced higher lung DC activation and promoted increased migration of lung DCs to the draining lymph nodes, resulting in increased numbers of virus-specific $CD8^+$ and $CD4^+$ T cells in the lungs compared with H1N1-infected mice. Despite greater numbers of virus-specific T cells, we observed delayed clearance of H5N1 from the lungs, which correlated with higher PD-1 expression and increased production of the anti-

inflammatory cytokine interleukin-10 (IL-10) by T cells in H5N1-infected mice. Importantly, we observed fewer numbers of virus-specific tissue-resident memory T cells in H5N1-infected mice compared with H1N1-infected mice. Taken together, our study demonstrates that hyperactivation of innate immune cells during H5N1 infection impairs cytotoxic T cell functions as well as subsequent generation of influenza virus-specific tissue-resident memory T cells.

RESULTS

H5N1 infection induces higher activation of innate immune cells. To establish if infection with a low-pathogenic H5N1 virus results in higher activation of innate immune cells, we infected C57BL/6 mice with a recombinant H5N1-green fluorescent protein (GFP) (A/Vietnam/1203/2004) or H1N1-GFP (A/Puerto Rico/8/1934, PR8 strain) virus and measured the activation status of different cell populations in the lungs by quantifying cell surface upregulation of CD86. For comparison, we utilized the mouse-adapted H1N1 (PR8) strain, as it replicates efficiently in murine lungs. We observed higher upregulation of CD86 on both types of lung-resident DCs ($CD103^+$ DC and CD11b+ DC) in mice infected with H5N1-GFP than that in mice infected with H1N1-GFP (Fig. 1A and B). In addition, we observed higher upregulation of CD86 on inflammatory DCs and inflammatory monocytes from H5N1-GFP-infected mice than from H1N1-GFP-infected mice, demonstrating that H5N1 infection results in higher activation of innate immune cells (Fig. 1C and D).

Next, to determine if the hemagglutinin (HA) and neuraminidase (NA) of H5N1 virus are sufficient to induce higher activation of innate immune cells, we generated a 2:6 reassortant virus carrying the HA and NA from H5N1 with the 6 internal genes of PR8 (H5N1 (2:6)) and compared it to the parental strain in subsequent studies. In this way, we can minimize the differences in viral replication between H5N1 and H1N1, as well as monitor T cell responses against the same epitopes in the internal viral genes. To confirm higher activation of innate immune cells by the H5N1 (2:6) reassortant strain, C57BL/6 mice were infected with H5N1 (2:6) or H1N1 and the levels of CD86 were analyzed by flow cytometry on day 2 postinfection (p.i.). In mice infected with H5N1 (2:6), we observed higher expression of CD86 on both types of lung-resident DCs ($CD103^+$ DC and CD11b+ DC) than that in H1N1-infected mice (Fig. 1E and F). In addition, we observed increased expression of interferon beta (IFN-β) and interferon-stimulated genes (ISGs) in the lungs of H5N1 (2:6)-infected mice on day 4 p.i. compared with H1N1-infected mice (Fig. 1G). Together, these results demonstrate that the HA and NA of H5N1 can induce higher innate immune responses in the lungs.

H5N1 (2:6) infection stimulates increased migration of lung DCs to the MLN. Upon acquisition of viral antigens and subsequent activation, lung DCs upregulate CCR7 and migrate to the mediastinal lymph nodes (MLNs) to prime naive T cells. To determine if hyperactivation of lung DCs alters their migration to the lymph nodes, we infected mice with H5N1 (2:6) or H1N1 and analyzed the levels of CCR7 upregulation by flow cytometry and monitored the levels of lung DC accumulation in the MLN via carboxyfluorescein succinimidyl ester (CFSE) labeling. We observed increased upregulation of CCR7 on the $CD103^+$ DC subset in H5N1 (2:6)-infected mice compared with H1N1-infected mice (Fig. 2A and B); however, CCR7 expression was comparable in the CD11b+ DC subset in both groups. Next, to determine the levels of lung DC migration to the MLN, we labeled cells in the respiratory tract by instilling CFSE dye on day 2 p.i. and measured the levels of CFSE-positive lung DCs in the MLN after 16 h. We observed an increased accumulation of CFSE+ lung DCs in the MLN of H5N1 (2:6)-infected mice compared with H1N1-infected mice (Fig. 2C to E). In addition, we observed increased numbers of total lung DCs in the MLN of H5N1 (2:6)-infected mice compared with H1N1-infected mice (Fig. 2E). These data demonstrate that H5N1 (2:6) infection induces higher activation of lung DCs, resulting in increased migration and accumulation of lung DCs in the MLN.

Mice infected with H5N1 (2:6) show robust activation of T cell responses but display delayed viral clearance. Next, we determined if the greater numbers of DCs

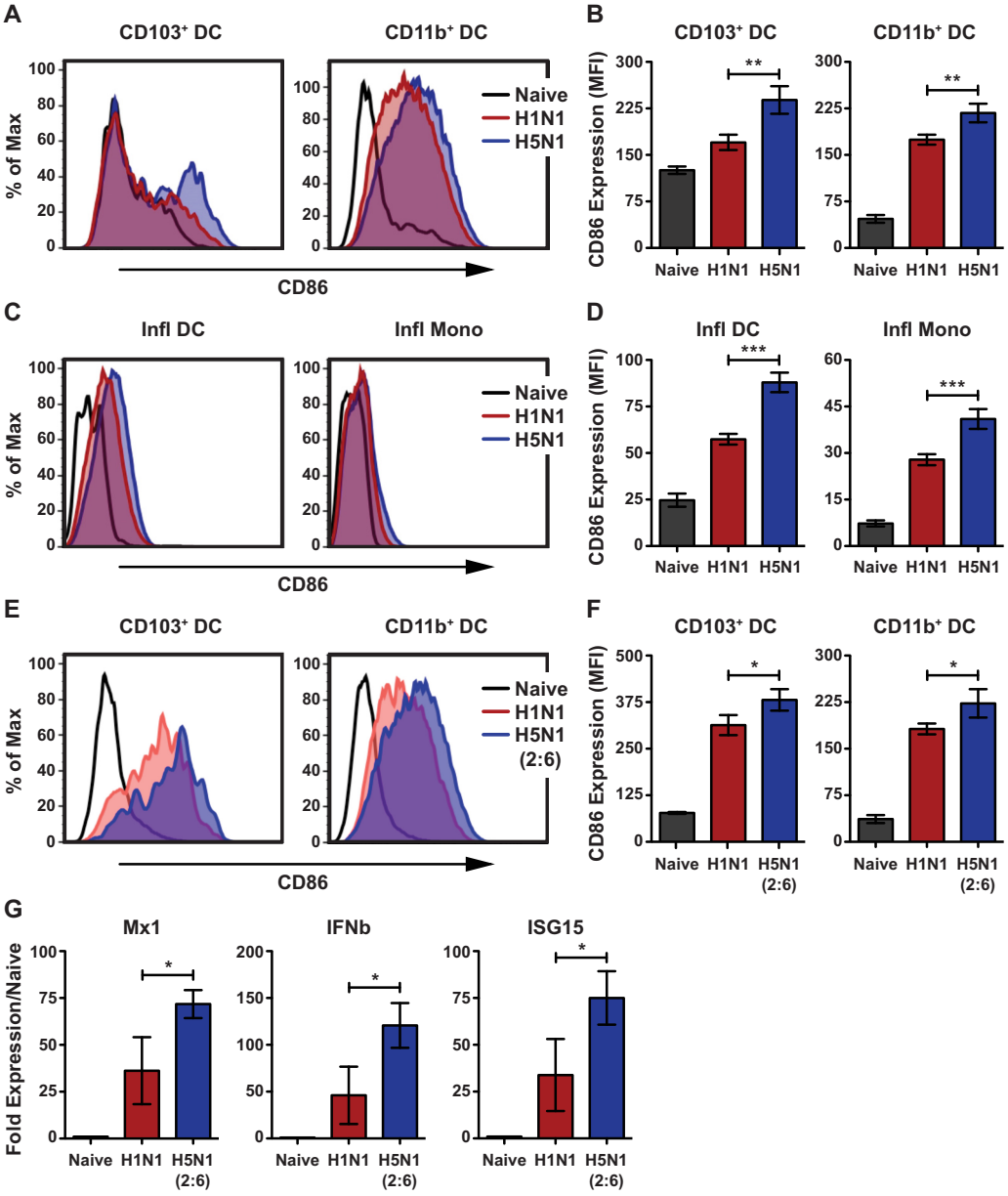

FIG 1 H5N1 virus stimulates higher activation of dendritic cells in the lungs. (A to D) C57BL/6 mice ($n = 3$ to 4 per group) were infected with 5×10^4 PFU of H1N1-GFP or H5N1-GFP, and cell surface expression of costimulatory molecule CD86 was measured flow cytometry. (A) Representative histograms comparing CD86 expression on lung DC subsets. (B) Quantification of CD86 expression on lung DC subsets. CD86 expression levels are shown as mean fluorescent intensity (MFI). (C and D) Comparison of CD86 expression on inflammatory DCs and monocytes. (C) Histogram plot of CD86 expression. (D) Quantification of CD86 expression. (E and F) Comparison of CD86 expression on DC subsets in mice infected with H5N1 (2:6) and H1N1. C57BL/6 mice were infected with 100 PFU of H1N1 or H5N1 (2:6), and CD86 expression was measured flow cytometry. (E) Representative histograms of CD86 expression on lung DC subsets. (F) Quantification for panel E shown as MFI. (G) Comparison of Mx1, ISG15, and IFN-β expressions between H5N1 (2:6)- and H1N1-infected lungs. Total RNA was extracted from lung homogenates of infected mice isolated on day 4 p.i. and subjected to reverse transcriptase quantitative PCR (qRT-PCR) analysis. The values are expressed as mean ± SD. *, **, and *** denote significance of <0.05, <0.01, and <0.001, respectively. Data are representative of at least three independent experiments.

observed in the MLN of H5N1 (2:6)-infected mice resulted in enhanced T cell responses and viral clearance. To evaluate primary T cell responses, C57BL/6 mice were infected with 100 PFU of H5N1 (2:6) or H1N1 and T cell responses were measured on day 8 p.i. by tetramer staining and by monitoring for cytokine production upon *ex vivo* stimulation. $CD8^+$ T cell responses against H5N1 and H1N1 viruses encompass many epitopes, and here, we investigated the T cell response against immunodominant

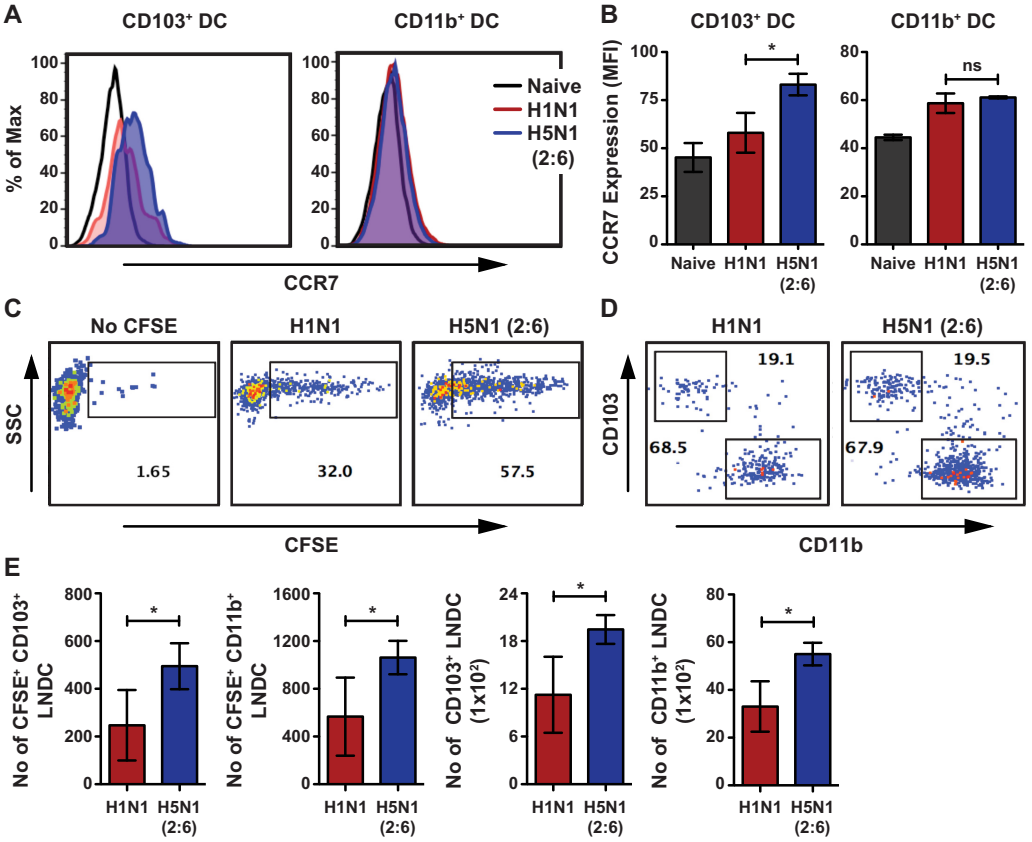

FIG 2 H5N1 (2:6) infection induces higher upregulation of CCR7 and migration of lung DCs. C57BL/6 mice ($n = 3$ to 4 per group) were intranasally infected with 100 PFU of H1N1 or H5N1 (2:6), and lung DC activation and migration were analyzed by flow cytometry. (A) Representative histogram comparing the expression of CCR7 on CD103$^+$ DC or CD11b+ DC subsets on day 2 p.i. (B) Quantification for panel A. CCR7 expression levels are shown as MFI. (C and D) C57BL/6 mice were infected with 100 PFU of H5N1 (2:6) or H1N1 and instilled with 50 μl of 8 mM CFSE at day 2 p.i. After 16 h, the number of CFSE+ migratory DC present in the MLN was analyzed by flow cytometry. (C) Representative FACS plots showing CFSE+ population in the MLN. (D) Relative levels of CFSE positive CD103$^+$ and CD11b+ DC in the MLN. (E) Bar charts showing the number of CFSE+ DC subsets in the MLN. (F) Bar chart showing total numbers of DC subsets in the MLN. The values are expressed as mean ± SD. * denotes statistical significance of <0.05; ns denotes not significant. Data are representative of at least two independent experiments.

epitopes (polymerase acidic [PA] and nucleocapsid protein [NP]) elicited in H5N1 (2:6) and H1N1 virus infections. Using tetramers specific for viral NP or PA, we observed increased frequencies of both NP and PA tetramer-positive CD8$^+$ T cells in H5N1 (2:6)-infected mice compared with H1N1-infected mice (Fig. 3A and B). The absolute numbers of NP and PA tetramer-positive CD8$^+$ T cells were also greater in H5N1(2:6)-infected mice than in H1N1-infected mice (Fig. 3C). In addition, *ex vivo* stimulation with X-31 (H3N2) virus or viral peptides showed increased frequencies of interferon gamma (IFN-γ)- and granzyme B (GrB)-producing CD8$^+$ T cells in H5N1 (2:6)-infected mice compared with H1N1-infected mice (Fig. 3D). Moreover, H5N1 (2:6)-infected mice showed increased frequencies of IFN-γ- and GrB-producing CD4$^+$ T cells compared with H1N1-infected mice (Fig. 3E). These results demonstrate that hyperactivated lung DCs promote robust activation of virus-specific T cell responses in the lung.

In the mouse model of influenza virus, innate immune cells restrict viral replication prior to the establishment of adaptive T cell responses. However, after day 6 p.i., T cells primed in the MLN migrate to the lungs and participate in the clearance of virus-infected cells. Therefore, we determined if the greater numbers of virus-specific T cells observed in H5N1 (2:6)-infected mice resulted in efficient viral clearance in the lungs. C57BL/6 mice were infected with 100 PFU of H5N1 (2:6) or H1N1; viral loads in the lungs were measured by plaque assay at various days p.i. Prior to and including day 6 p.i., we

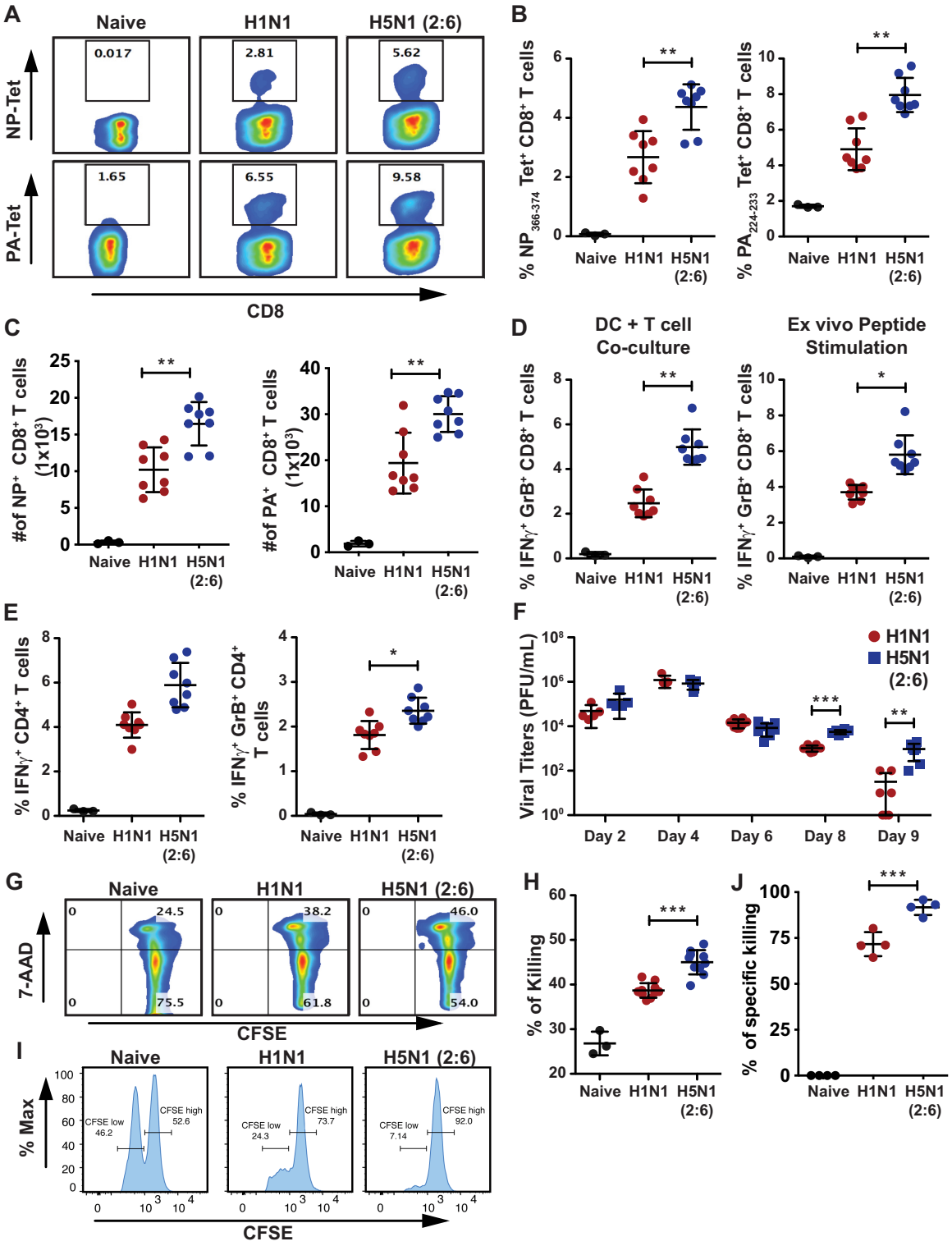

FIG 3 Mice infected with H5N1 (2:6) mount robust T cell responses but show delayed viral clearance. (A to E) C57BL/6 mice ($n = 3$ to 4/group) were infected with 100 PFU of H1N1 or H5N1 (2:6), and on day 8 p.i., T cells from the lungs were isolated and evaluated in various assays. (A to C) Comparative analysis of lung CD8$^+$ T cells from H5N1 (2:6)- or H1N1-infected mice by NP or PA tetramer staining. (A) Representative FACS plots for NP or PA tetramer staining. (B) Relative frequency of tetramer positive CD8$^+$ T cells. (C) Absolute numbers of NP or PA tetramers positive CD8$^+$ T cells. (D and E) Comparative analysis of cytokine production in T cells isolated from the lungs of H5N1 (2:6)- or H1N1-infected mice. T cells were cocultured with BMDCs either infected with X31 (H3N2) or pulsed with NP peptide, and the frequencies of IFN-γ- and GrB-producing T cells were analyzed by flow cytometry. (D) Relative frequency of cytokine-producing CD8$^+$ T cells. (E) Relative frequency of cytokine-producing CD4$^+$ T cells stimulated with NP peptide. (F) Evaluation of viral loads in the lungs of infected mice. C57BL/6 mice were infected with 100 PFU of H1N1 or H5N1 (2:6) and at various times p.i., viral loads in the lungs were

(Continued on next page)

observed similar viral loads in the lungs of both groups of infected mice, suggesting that both viruses replicate to similar levels (Fig. 3F). However, on day 8 and day 9 p.i., we observed greater viral loads (~5- to 10-fold) in the lungs of H5N1 (2:6)-infected mice than that of H1N1-infected mice. These results demonstrate that, despite the presence of more virus-specific T cells in the lungs, viral clearance was delayed in H5N1 (2:6)-infected mice.

To understand the basis for the delayed clearance of H5N1 (2:6) in the lungs, we evaluated the functionality of T cells by *in vitro* T cell killing assay. In this assay, T cells isolated from H5N1 (2:6) or H1N1-infected mice were cocultured with CFSE-labeled splenocytes pulsed with the NP peptide, and the amount of target cell death was determined by quantification of 7-aminoactinomycin D (7-AAD)-positive splenocytes. Interestingly, we observed more splenocyte death in cocultures containing T cells from H5N1 (2:6)-infected mice than in cocultures containing T cells from H1N1-infected mice (Fig. 3G and H). Next, we performed an *in vivo* killing assay with peptide-pulsed splenocytes. Splenocytes were labeled with either low CFSE or high CFSE and pulsed with influenza virus NP peptide or control peptide, respectively. Splenocytes were adoptively transferred into mice previously infected with either H5N1(2:6) or H1N1 (day 8 p.i.) (Fig. 3I and J) and 8-h post-adoptive transfer mice splenocytes were analyzed for CFSE+ cells. Our data demonstrate that cytotoxic T cells from H5N1 (2:6)-infected mice can effectively kill peptide-pulsed splenocytes both *in vitro* and *in vivo*.

Cytotoxic T cells from H5N1 (2:6)-infected mice show higher expression of PD-1 and IL-10. T cell functions can be modulated by stimulatory as well as inhibitory signals. Prior studies demonstrate that during influenza virus infection, T cell functions can be suppressed by PD-1/PD-L1 interactions and by the anti-inflammatory cytokine IL-10 (30–32). In addition, PD-1 has shown to be upregulated in T cells in response to direct activation of T cell receptor (TCR). Although the T cells isolated from H5N1 (2:6)-infected mice were efficient in killing peptide-pulsed splenocytes, we observed delayed viral clearance in the lungs (Fig. 3F and G). Thus, we investigated if the T cell functionality was suppressed *in vivo* through PD-1/PD-L1 interactions by measuring the expression of PD-1/PD-L1 by flow cytometry. We observed significantly higher levels of PD-1 on $CD8^+$ T cells isolated from H5N1 (2:6)-infected mice than that from H1N1-infected mice (Fig. 4A and B). Next, we analyzed different cellular compartments in the lungs for PD-L1 expression and observed significantly higher levels of PD-L1 on inflammatory monocytes (CD11b+ $Ly6C^{hi}$ $Ly6G^-$) isolated from H5N1 (2:6)-infected mice than that from H1N1-infected mice (Fig. 4C). In addition, we observed increased numbers of inflammatory monocytes in the H5N1(2:6)-infected mice group (Fig. 4D). However, the levels of PD-L1 on other cellular compartments in the lungs, including inflammatory DCs were similar between the two groups. Next, we measured IL-10 production in T cells isolated from infected mice to determine the possibility of IL-10-mediated suppression of T cell functions. T cells isolated from H5N1 (2:6) or H1N1-infected mice on day 8 p.i. were cocultured with DCs pulsed with the major histocompatibility complex class I (MHC-I) or MHC-II peptide or infected with X-31 (H3N2) virus, and the production of IFN-γ and IL-10 in T cells was measured by flow cytometry. We observed an increased production of IFN-γ and IL-10 in both $CD8^+$ and $CD4^+$ T cells isolated from H5N1 (2:6)-infected mice compared with H1N1-infected mice (Fig. 4E and F). Taken together, these results demonstrate that H5N1 (2:6) infection results in higher expression of inhibitory signals such as PD-1 and IL-10 by T cells, which likely suppress cytotoxic T cell functions *in vivo*.

FIG 3 Legend (Continued)
measured by standard plaque assay. (G and H) *Ex vivo* analysis of cytotoxic T cell functions. CFSE-labeled splenocytes pulsed with NP peptide were cocultured with lung $CD8^+$ T cells for 8 h, followed by staining with 7-AAD. *Ex vivo* cytotoxic effects of $CD8^+$ T cells were evaluated by analyzing 7-AAD-positive splenocytes. Representative FACS plots for 7-AAD-positive cells (G) and relative level of killing by T cells shown as percentage of 7-AAD positive cells (H). (I and J) *In vivo* analysis of cytotoxic T cell functions. Representative FACS plots for *in vivo* killing of adoptively transferred NP-pulsed splenocytes in H1N1 virus- or H5N1 (2:6) virus-infected mice (I) and relative level of killing by T cells (J). The values are expressed as mean ± SD. *, **, and *** denote significance of <0.05, <0.01, and <0.001, respectively. Data in panels A to F are from two independent experiments pooled. Data in panels G to J are from one experiment.

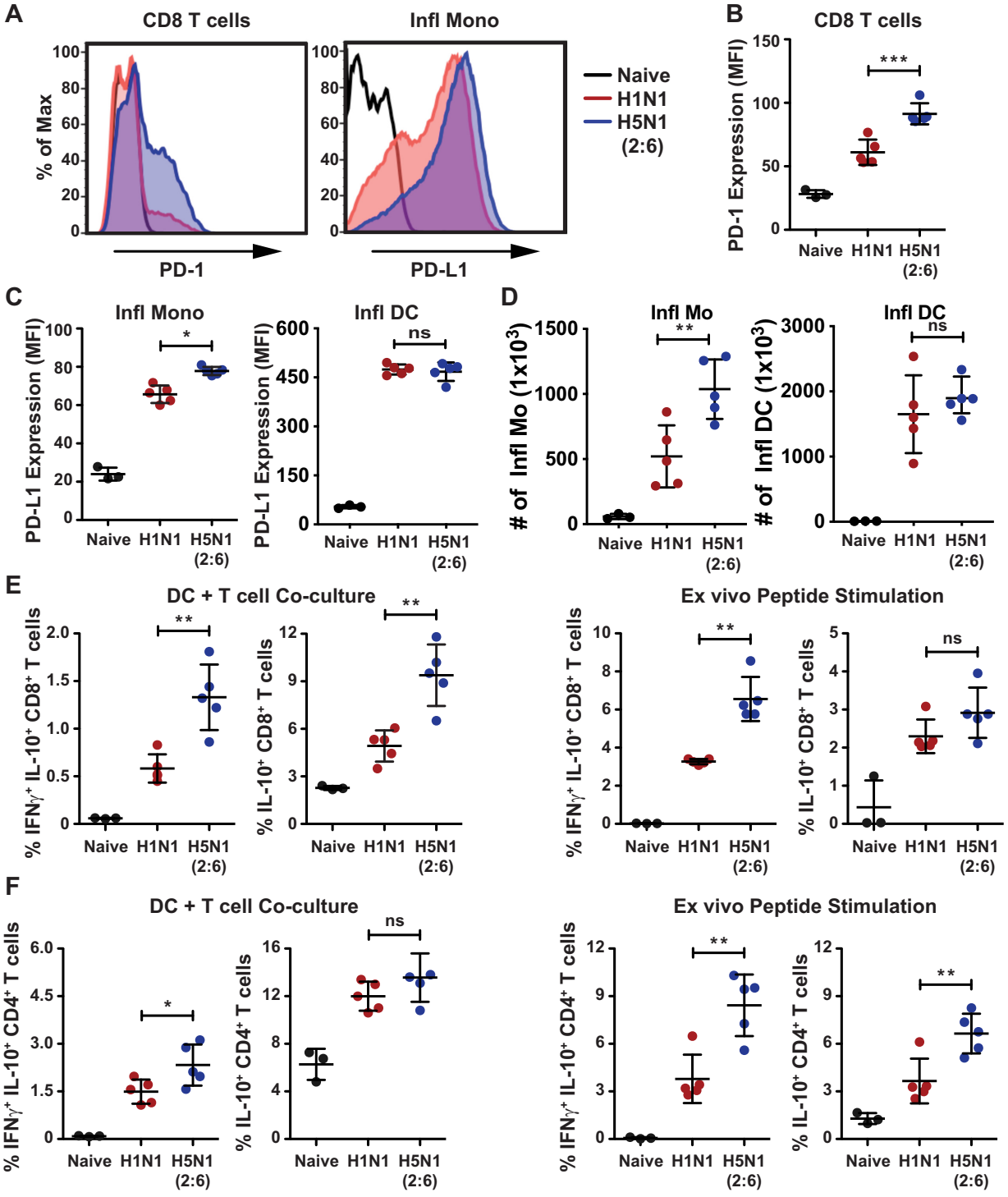

FIG 4 H5N1 (2:6) infection induces higher expression of PD-1 and IL-10 in cytotoxic T cells. C57BL/6 mice were infected with H5N1 (2:6) or H1N1 virus, and on day 8 p.i., expression of PD-1 and production of IL-10 in $CD8^+$ T cells were measured *ex vivo* upon coculture with infected DCs or peptide-pulsed DCs by flow cytometry. PD-L1 expression on inflammatory monocytes was also measured by flow cytometry. (A) Representative histograms showing expression of PD-1 on $CD8^+$ T cells and PD-L1 on $Ly6C^+$ inflammatory monocytes. (B) Quantification for PD-1 expression in CD8 T cells as MFI. (C) Quantification of PD-L1 expression in inflammatory monocytes and inflammatory DCs. (D) Absolute numbers of inflammatory monocytes and inflammatory DCs. (E) Quantification of IL-10-producing $CD8^+$ T cell frequencies in X-31-infected DC-T cell coculture (top panel) and NP peptide-pulsed DC-T cell coculture (bottom panel). (F) Cytokine production in $CD4^+$ T cells. Frequencies of IFN-γ and IL-10 or IL-10 alone producing $CD4^+$ T cells in X-31-infected DC-T cell coculture (left panels) and NP peptide-pulsed DC-T cell coculture (right panels). The values are expressed as mean ± SD. *, **, and *** denote significance of <0.05, <0.01, and <0.001, respectively.

H5N1-infected mice show decreased numbers of memory T cells in the lung parenchyma. Upon clearance of viral infection, a portion of virus-specific T cells differentiate into tissue-resident memory T (T_{RM}) cells, which play an important role in providing heterosubtypic immunity against subsequent influenza virus infections (33). As we observed higher upregulation of inhibitory signals (PD-1 and IL-10) on T cells from H5N1 (2:6)-infected mice, we investigated if T_{RM} cell responses were also impaired. Previously, T_{RM} cells in lungs post-influenza virus infection have been characterized with the expression of CD69 and CD103 on day 30 p.i. (34). We analyzed the lung parenchyma for memory T cells that exhibit the T_{RM} cell phenotype ($CD69^+$ $CD44^+$ $CD103^+$) by flow cytometry (35, 36). Circulating T cells were excluded by intravenous injection of labeled anti-CD8β antibody prior to euthanizing mice and excluding this population from analysis (gating strategy shown in Fig. 5A). We observed fewer numbers of NP tetramer-positive $CD8^+$ T_{RM} cells in the lungs of H5N1 (2:6)-infected mice than that in H1N1-infected mice (Fig. 5B). Similarly, the numbers of $CD4^+$ T_{RM} cells were fewer in H5N1 (2:6)-infected mice than in H1N1-infected mice (Fig. 5C). These results demonstrate that H5N1 (2:6) infection results in decreased differentiation of lung-resident memory T cells. Next, to determine if the fewer numbers of tissue-resident memory cells affect protection from future challenge, C57BL/6 mice were infected with 50 PFU of H1N1 or H5N1(2:6) virus and were subsequently challenged with a heterologous H3N2 strain (X-31), a reassortant strain that share 6 internal genes with H1N1 and H5N1(2:6) viruses (Fig. 5D). We did not observe significant differences in weight loss between H1N1- and H5N1 (2:6)-infected groups upon lethal challenge with the H3N2 (X-31) strain. These data suggest that the lowered levels of memory T cells in H5N1 (2:6) infection do not impact protection against heterologous strains.

DISCUSSION

Infections with avian H5N1 influenza virus induce higher innate immune responses than human H1N1 viruses (21, 37). However, due to inherent differences in replication levels, it is difficult to discern if this hyperactivation of innate immune responses against H5N1 is due to higher viral replication in the lungs. To overcome this caveat, we generated an H5N1 strain sharing the 6 internal genes of H1N1 (H5N1 (2:6)) and observed that the HA and NA of H5N1 can induce higher activation of lung DCs. As such, this heightened stimulation of lung DCs by H5N1 (2:6) resulted in increased migration of DCs to the MLN and induced robust T cell responses compared with H1N1 virus. Interestingly, despite the greater numbers of virus-specific T cells in the lungs, we observed delayed clearance of H5N1 (2:6) from the lungs of infected mice. This delayed viral clearance correlated with increased levels of PD-1 expression and IL-10 production by $CD8^+$ T cells, which likely suppress cytotoxic T cell functions *in vivo*. Importantly, H5N1 (2:6) infection resulted in decreased numbers of tissue-resident memory T cells compared with H1N1 infection. Taken together, our studies demonstrate that hyperactivation of the innate immune system by H5N1 (2:6) results in suppression T cell functions, delayed viral clearance, and decreased numbers of tissue-resident memory T cells.

Unlike seasonal influenza viruses, avian H5N1 influenza viruses can cause severe and often fatal disease in healthy individuals (38, 39). H5N1 infection induces uncontrolled activation of the host immune system, with heightened cytokine levels in the lungs as well as massive infiltration of neutrophils, inflammatory monocytes, and inflammatory tumor necrosis factor alpha/inducible nitric oxide synthase (TNF-α/iNOS)-producing (Tip) DCs (40). These infiltrating cells have been implicated in the enhanced virulence of avian H5N1 influenza viruses (26, 27, 40). Moreover, *ex vivo* studies show that H5N1 viruses induce higher human DC activation than H1N1 viruses (25). Similarly, our studies with H5N1 (2:6) virus demonstrated increased activation of murine lung DC compared with H1N1 virus, further suggesting that the H5N1 HA/NA are sufficient for higher activation of innate immune cells in the lungs (Fig. 1E and F). This increased activation of lung DCs in H5N1 (2:6)-infected mice was not due to differences in viral replication between strains, as both the reassortant H5N1 (2:6) and H1N1 (PR8) strains showed

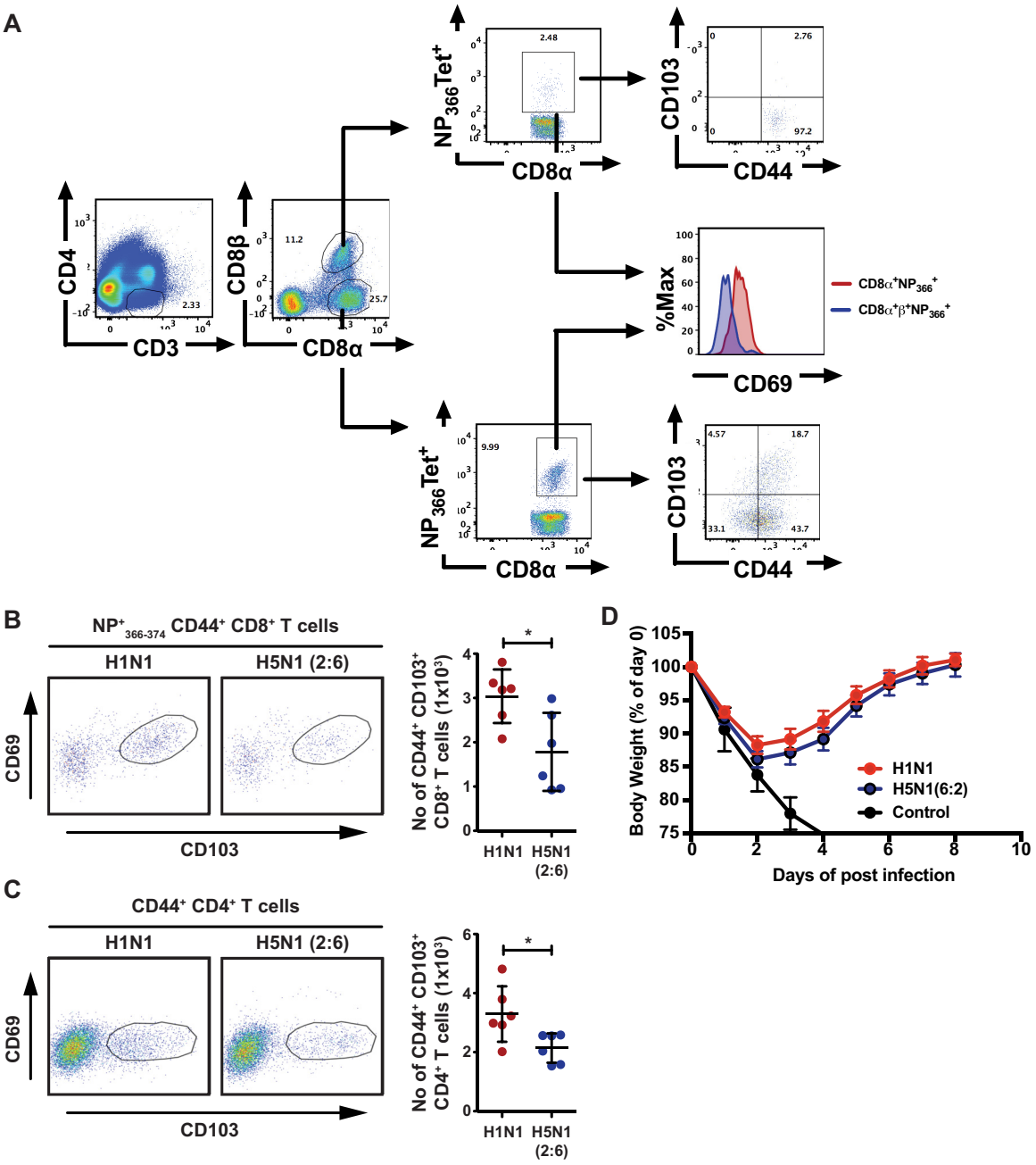

FIG 5 H5N1 (2:6) infection results in decreased numbers of tissue-resident memory T cells in the lung parenchyma. C57BL/6 mice ($n = 3$) were infected with H5N1 (2:6) or H1N1 virus, and on day 30 p.i., the frequency and absolute number of lung-resident memory cells was analyzed by flow cytometry. (A) Gating strategy for identifying tissue-resident memory T cells. (B) Lung-resident memory $CD8^+$ T cell responses. Representative FACS plots for lung-resident memory $CD8^+$ T cells (gated on $NP^+_{366\text{-}374}$ $CD44^+$ $CD8\alpha+$ $CD8\beta$-T cells) that display $CD44^+$ $CD69^+$ $CD103^{hi}$ phenotype (left) and the absolute numbers of tissue resident memory $CD8^+$ T cells (right). (C) Lung-resident memory $CD4^+$ T cell responses. Representative FACS plots (left) and absolute numbers of $CD4^+$ T cells (right) are shown. (D) Heterologous challenges with H3N2 (X-31) virus. Mice previously infected with 50 PFU of H1N1 or H5N2 (2:6) virus were challenged with the H3N2 (X-31) strain at a dose of 5×10^6 PFU. The values are expressed as mean ± SD. * denotes statistical significance of <0.05. Data in panels A and B are from two independent experiments pooled. Data in panel C were from one experiment.

similar levels of viral replication on days 2, 4, and 6 p.i. (Fig. 3F). These results corroborate prior *ex vivo* studies which indicate that viruses with different HA subtypes can differentially activate primary DCs and macrophages (41). However, the consequence of higher DC activation *in vivo* to subsequent adaptive immune responses was previously unknown. Our studies demonstrated that H5N1 (2:6) infection stimulated increased migration and accumulation of DCs in the MLN, resulting in robust T cell responses in

the lungs (Fig. 2C to E). Moreover, we observed increased frequencies of cytokine-producing T cells in H5N1 (2:6)-infected mice compared with H1N1-infected mice (Fig. 3). Together, these data demonstrate that hyperactivation of lung DCs results in increased numbers of virus-specific T cells in the lungs of H5N1 (2:6)-infected mice.

Prior studies demonstrate that the magnitude and the quality of T cell responses determine the efficiency of viral clearance (42). Previously, we demonstrated that mice deficient in retinoic acid inducible gene I (RIG-I) or mitochondrial antiviral signaling protein (MAVS) mounted poor T cell responses against influenza virus, as evidenced by decreased numbers of polyfunctional T cells and delayed viral clearance in the lungs (29). In contrast, despite mounting robust T cell responses, H5N1 (2:6)-infected mice showed delayed viral clearance in the lungs compared with H1N1-infected mice (Fig. 3F). This delayed viral clearance in H5N1 (2:6)-infected mice was likely due to active suppression of cytotoxic T cell functions *in vivo*, as T cells isolated from H5N1 (2:6)-infected mice showed efficient cytotoxic activity against NP peptide-pulsed splenocytes (Fig. 3G). In corroboration, we observed higher levels of inhibitory signals (PD-1 and IL-10) that likely suppress cytotoxic T cell functions *in vivo* and delay viral clearance (Fig. 4A and 3F). In our *in vivo* killing assays, H5N1 (2:6)-infected mice showed robust killing of viral peptide-loaded splenocytes, suggesting that inhibition of T cells may occur by direct suppression by cell-to-cell contact rather than by the presence of suppressive cytokine milieu. Prior studies indicate that infection with the lethal mouse-adapted PR8 strain (H1N1) resulted in higher PD-1 expression on T cells than the less-virulent X-31 (H3N2) reassortant strain (30). Interestingly, our studies show that infection with H5N1 reassortant (2:6) induced higher PD-1 expression than PR8 (H1N1) (Fig. 4A). As H5N1 viruses have been shown to have broad tissue tropism, it is possible that the increased PD-1 expression observed in H5N1 (2:6)-infected mice is likely due to antigen persistence and/or prolonged stimulation of T cells. PD-1 interactions with PD-L1 have been demonstrated to suppress cytotoxic $CD8^+$ T cell functions (43–45). PD-L1 expression is induced during viral infection on a variety of cell types, including monocytes, DCs, macrophages, and epithelial cells (44–47). In our analysis of cell types expressing PD-L1, we observed higher PD-L1 expression on $Ly6C^{hi}$ inflammatory monocytes isolated from H5N1 (2:6)-infected mice than that from H1N1-infected mice (Fig. 4C). In addition, the numbers of inflammatory monocytes were higher in H5N1(2:6)-infected mice than in H1N1-infected mice. It should be noted that PD-L1 expression was observed on others cell types as well; yet, there was no significant difference in PD-L1 levels between the two groups (data shown for inflammatory DCs) (Fig. 4C). In a prior study, anti-PD-L1 treatment of PR8-infected mice showed increased virus-specific T cells and decreased viral titers (30); however, anti-PD-L1 treatment did not alter disease outcome, suggesting that there may be additional mechanisms for suppression of T cell functions. In agreement, we observed an increased expression of the anti-inflammatory cytokine IL-10 in T cells isolated from H5N1 (2:6)-infected mice compared with H1N1-infected mice (Fig. 4C to E). Taken together, our data suggest that higher levels of IL-10 production and PD-1/PD-L1-mediated inhibition likely contribute to suppression of T cell functions and consequently results in delayed clearance of H5N1 (2:6) in the lungs.

Upon viral clearance in the lungs, a portion of virus-specific T cells differentiate into tissue-resident memory T cells, and these T_{RM} cells are critical for providing heterosubtypic immunity (36, 48). Interestingly, we observed decreased numbers of T_{RM} cells in H5N1 (2:6)-infected mice compared with H1N1-infected mice (Fig. 5). It should be noted that despite the decreased number of T_{RM} cells, we did not observe significant differences in protection against challenge from a heterologous H3N2 strain. Our future studies will determine if fewer numbers of T_{RM} cells are due to defects in differentiation versus maintenance of T_{RM} cells. Prior studies indicate that transforming growth factor-β (TGF-β) promotes maturation of T_{RM} by inducing the upregulation of CD103 expression (36, 49–51). Coincidently, influenza viral neuraminidase (NA) can convert latent TGF-β into mature TGF-β; however, the NA of H5N1 is unable to activate TGF-β both *in vitro* and *in vivo* (52, 53). It is possible that the decreased numbers of T_{RM} cells in H5N1 (2:6)-infected mice may result from lowered levels of TGF-β activation by viral

NA. Apart from TGF-β, interleukin-33 (IL-33) and tumor necrosis factor (TNF) are also known to induce T_{RM} cell-like phenotypes ($CD69^+$ $CD103^+$) (36, 49–51). Moreover, homeostatic cytokine IL-15 is required for T_{RM} cell differentiation and survival (36). Thus, it is also possible that H5N1 (2:6) infections may alter the levels of other cytokines that are critical for the generation and maintenance of T_{RM} cells. Alternatively, sustained inflammation during H5N1 (2:6) infection may negatively regulate T_{RM} cell differentiation due to higher levels of IFN-β and IL-12 (54). Further studies are needed to determine if decreased TGF-β levels or sustained higher inflammation in the lungs of H5N1 (2:6)-infected mice are responsible for the inefficient differentiation of the T_{RM} population.

In conclusion, our study demonstrates that hyperactivation of innate immune cells by H5N1 (2:6) dampens T cell responses and delays viral clearance in the lungs. This is likely due to higher expression of the inhibitory molecule PD-1 on T cells as well as higher production of the anti-inflammatory cytokine IL-10 by T cells in H5N1 (2:6)-infected mice. As such, our studies show that suppression of T cell responses may contribute to the protracted viral replication and prolonged illness associated with avian influenza virus infection in humans.

MATERIALS AND METHODS

Ethics statement. All studies were performed in accordance with the principles described by the Animal Welfare Act and the National Institutes of Health guidelines for the care and use of laboratory animals in biomedical research. The protocols for performing murine studies were reviewed and approved by the Institutional Animal Care and Use Committee (IACUC) at the University of Chicago.

Cell lines. Human embryonic kidney cells (293T; ATCC) were maintained in Dulbecco's modified Eagle's medium (DMEM; Gibco) supplemented with 10% fetal bovine serum (FBS; Denville Scientific) and penicillin/streptomycin (pen/strep; 100 units/ml; Corning). Madin-Darby canine kidney (MDCK; ATCC) cells were maintained in minimum essential medium (MEM; Lonza) supplemented with 10% FBS and pen/strep (100 units/ml).

Viruses. The generation of H1N1-GFP (A/Puerto Rico/8/1934) was described earlier (55). H5N1-GFP (A/Vietnam/1203/2004; low pathogenic without the multibasic site in HA), which contains a GFP reporter in the NS segment, was generated following a similar protocol (55). H5N1 (2:6) (A/Vietnam/1203/2004; low pathogenic without the multibasic site in HA), which contains the 6 internal genes from the PR8 strain, was rescued using standard reverse genetics techniques (55, 56). Briefly, 0.5 μg of each of the six pDZ plasmids representing PB2, PB1, PA, NP, NS, and M from A/Puerto Rico/8/1934 (PR8) and two pPol-I plasmids representing the HA (low pathogenic) and NA segments of H5N1 were transfected into a cell mixture containing 293T-MDCK using Lipofectamine 2000 (Invitrogen). After 48 h, 200 μl of the rescue supernatants was used to infect fresh MDCK cells seeded in 6-well plates. The successful rescue of recombinant viruses was confirmed by performing a hemagglutination assay with chicken red blood cells. After plaque purification, the recombinant viruses were amplified in 10-day-old specific-pathogen-free eggs (Charles River). Viral titers were determined by plaque assay in MDCK cells using standard techniques.

Mice infection. C57BL/6 mice were purchased from Jackson Laboratory and bred in specific-pathogen-free (SPF) facilities maintained by the University of Chicago Animal Resource Centre. All experiments were performed with gender-matched mice of 6 to 8 weeks of age. For influenza virus infections, mice were anesthetized with ketamine/xylazine (intraperitoneally [i.p.]; 80/10 mg/kg) and infected intranasally with the indicated dose of virus diluted in 25 μl of phosphate-buffered saline (PBS).

Reverse transcriptase quantitative PCR analysis. Total RNA from lung tissue was extracted using TRIzol (Life technologies) following the manufacturer's instructions, and cDNA was synthesized with SuperScript II using oligo dT primers (Roche Diagnostics). Quantitative PCR was performed using previously described gene-specific primers in an ABI 7300 real-time PCR system with SYBR green master mix (Invitrogen) (12).

Flow cytometric analyses. Preparation of lung samples for flow cytometric analysis and T cell assays were performed following techniques we previously described (29). Briefly, after euthanization, murine lungs were perfused with 10 ml of PBS, excised and finely chopped with scissors, and digested in 0.4 mg of collagenase in Hanks' balanced salt solution (HBSS)/10% FBS for 45 minutes at 37°C. Mediastinal lymph nodes (MLNs) were carefully isolated and digested in 0.2 mg of collagenase in HBSS/10% FBS for 15 minutes at 37°C. To prepare single-cell suspensions, collagenase-treated lung tissues and MLNs were passed through a 19-G blunt needle a few times and filtered through a 70-μm cell strainer. After two washes in fluorescence-activated cell sorter (FACS) buffer (PBS containing 1% FBS and 2 mM EDTA), the cells were subjected to red blood cell (RBC) lysis (Biowhitaker) for 3 minutes followed by two washes with FACS buffer. The single-cell preparations were resuspended in FACS buffer containing 10 μg/ml Fc receptor block and incubated for 15 minutes. For DC subset analysis, lymph node and lung cells were stained with antibodies against the following multiple surface antigens: anti-CD45 (2 μg/ml; clone 30-F11; BioLegend), anti-SiglecF (1 μg/ml; clone E50-2440; BD Biosciences), anti-CD11c (2 μg/ml; clone N418; BioLegend), anti-MHC-II (2 μg/ml; clone M5/114.15.2; BioLegend), anti-CD103 (2 μg/ml; clone 2E7; eBiosciences), anti-CD11b (1 μg/ml; clone M1/70; BioLegend), anti-CD86 (2 μg/ml; clone GL-1;

BioLegend), anti-Ly6G (1 μg/ml; clone 1A8; BioLegend), anti-Ly6C (2 μg/ml; clone HK1.4; BioLegend), anti-CD4 (2 μg/ml; clone RM4-4; BioLegend), anti-CD3 (2 μg/ml; clone 145-2C11; eBiosciences), and anti-CD8 (1 μg/ml; clone 53-6.7; eBiosciences). Dead cells were stained with Live/Dead fixable near-infrared (IR) staining kit (Life Technologies) in PBS for 15 min on ice. Surface-stained samples were fixed with FACS buffer containing 0.1% formaldehyde and analyzed using the BD LSR-II flow cytometer. Data analysis was performed using FlowJo software (Treestar Corp.).

DC and T cell assays. Bone-marrow-derived dendritic cells (BMDCs) were generated from C57BL/6 mice, and T cell restimulation experiments were performed as previously described (57, 58). Briefly, BMDCs were infected with X-31 (H3N2) at a multiplicity of infection (MOI) of 0.5 for 5 h, washed with PBS 3 times to remove unbound virus, and resuspended in Iscove's modified Dulbecco's medium (IMDM) with 10% FBS (Invitrogen). T cells from the lungs of naive or infected mice (day 8 p.i.) were enriched using the Pan T cell isolation kit II (Miltenyi Biotec) and cocultured with infected BMDCs at a ratio of 10:1 for 2 to 3 h, followed by the addition of brefeldin A (5 μg/ml; eBiosciences). The cells were further incubated for an additional 8 to 10 h at 37°C. *Ex vivo* peptide stimulation studies were performed using MHC-I $NP_{366-374}$ (ASNENMETM) or MHC-II-restricted $NP_{311-325}$ (QVYSLIRPNENPAHK) peptides. The cells were first stained for cell surface markers as described above, followed by intracellular staining for cytokines. For intracellular staining, cells were incubated in permeabilization and fixation buffer (BD Pharmingen) for 45 minutes, followed by 2 washes in a PBS buffer containing 1% FBS and 0.5% saponin (Sigma, St. Louis, MO). Intracellular staining for anti-IFN-γ (2 μg/ml; clone XMG1.2; BioLegend), anti-granzyme B (2 μg/ml; clone GB11; BioLegend), and IL-10 (2 μg/ml; clone JES5-16E3; BioLegend) was performed on ice for 30 minutes.

For T cell tetramer staining, lymphocytes from the lungs of influenza virus-infected mice were enriched using Ficoll-Hypaque (GE Healthcare Life Sciences) density gradient and stained with H-$2D^b$ restricted tetramers conjugated to fluorophore R-phycoerythrin (PE) ($NP_{366-374}$ ASNENMETM or $PA_{224-233}$ SSLENFRAYV).

***In vivo* killing assay.** Single-cell suspension was prepared from mice spleen, and the cells were pulsed either with 1 μM $NP_{366-374}$ peptide or OT-1 peptide ($Ova_{257-264}$) for 1 h and labeled with 1 μM CFSE ($CFSE^{low}$) or 5 μM CFSE ($CFSE^{high}$), respectively, following manufacturer's instructions (Life Technologies). A mixture of 2×10^6 $CFSE^{low}$ and $CFSE^{high}$ splenocytes were intravenously injected to gender-matched naive mice or the mice which had been intranasally infected 8 days ago with H1N1 or H5N1 (2:6) virus. After 5 h of injection, mice splenocytes were analyzed for CFSE-positive cells by flow cytometry. Percent killing was determined using the following equation: % specific lysis = 100 − [100 × (% $CFSE^{low}$ infected mouse/% $CFSE^{high}$ infected mouse)/(% $CFSE^{low}$ naive mouse/% $CFSE^{high}$ naive mouse).

Analysis of tissue-resident memory T cells. Lung-resident memory $CD8^+$ T cells were analyzed as previously described (34). Mice were intranasally infected with H1N1 or H5N1 (2:6) virus. On day 30 postinfection, mice were intravenously injected with 1 μg anti-CD8β antibody 5 minutes before tissue harvest. Lung tissues were perfused with PBS and single-cell suspensions were prepared after digestion with collagenase as described before. Cells were blocked first with FcRγIII/II antibody and stained with H-$2D^b$ restricted tetramer conjugated to fluorophore R-phycoerythrin (PE) ($NP_{366-374}$ ASNENMETM). Tetramer-labeled cells were washed and stained with anti-CD4 (2 μg/ml; clone RM4-4; BioLegend), anti-CD3 (2 μg/ml; clone 145-2C11; eBiosciences), anti-CD8a (1 μg/ml; clone 53-6.7; eBiosciences), anti-CD44 (clone IM7; BioLegend), anti-CD103 (2 μg/ml; clone 2E7; eBiosciences), and anti-CD69 (clone H1.2F3; BioLegend). Dead cells were stained with the Live/Dead fixable near-IR staining kit (Life Technologies) in PBS for 15 minutes on ice. Surface-stained samples were fixed with FACS buffer containing 0.1% formaldehyde and analyzed using the BD LSR-II flow cytometer. Data analysis was performed using FlowJo software (Treestar Corp.).

Statistical analysis. Data were analyzed using Prism GraphPad software, and statistical significance was determined by one-way analysis of variance (ANOVA) or the unpaired Student's *t* test. *, **, and *** denote significance of <0.05, <0.01, and <0.001, respectively; ns denotes not significant.

ACKNOWLEDGMENTS

We are grateful to Adolfo García-Sastre at the Icahn School of Medicine for providing numerous reagents used in this study. H5N1 reverse genetics plasmids were kindly provided by John Steel at Emory University. We thank the NIH Tetramer Core Facility at Emory University for providing us with influenza virus-specific T cell tetramers. We also thank the staff at the Office of Research Safety and the Animal Resource Center at the University of Chicago for their excellent support.

M.K., B.M., and S.M. conceived and designed the study. M.K., K.F., and S.M. performed experiments. M.K., J.T.P., S.M., and B.M. wrote the manuscript. All authors approved the manuscript.

REFERENCES

1. Palese P, Shaw ML. 2007. Orthomyxoviridae: the viruses and their replication, p 1647–1689. *In* Knipe DM, Howley PM, Griffin DE, Lamb RA, Martin MA, Roizman B, Straus SE (ed), Fields virology, 5th ed. Lippincott Williams & Wilkins, Philadelphia, PA.
2. Nair H, Brooks WA, Katz M, Roca A, Berkley JA, Madhi SA, Simmerman JM, Gordon A, Sato M, Howie S, Krishnan A, Ope M, Lindblade KA, Carosone-Link P, Lucero M, Ochieng W, Kamimoto L, Dueger E, Bhat N, Vong S, Theodoratou E, Chittaganpitch M, Chimah O, Balmaseda A, Buchy P,

Harris E, Evans V, Katayose M, Gaur B, O'Callaghan-Gordo C, Goswami D, Arvelo W, Venter M, Briese T, Tokarz R, Widdowson M-A, Mounts AW, Breiman RF, Feikin DR, Klugman KP, Olsen SJ, Gessner BD, Wright PF, Rudan I, Broor S, Simões EAF, Campbell H. 2011. Global burden of respiratory infections due to seasonal influenza in young children: a systematic review and meta-analysis. Lancet 378:1917–1930. https://doi.org/10.1016/S0140-6736(11)61051-9.

3. Thompson WW, Shay DK, Weintraub E, Brammer L, Cox N, Anderson LJ, Fukuda K. 2003. Mortality associated with influenza and respiratory syncytial virus in the United States. JAMA 289:179–186. https://doi.org/10.1001/jama.289.2.179.
4. Webster RG, Bean WJ, Gorman OT, Chambers TM, Kawaoka Y. 1992. Evolution and ecology of influenza A viruses. Microbiol Rev 56:152–179. https://doi.org/10.1128/MMBR.56.1.152-179.1992.
5. Vincent AL, Ma W, Lager KM, Janke BH, Richt JA. 2008. Swine influenza viruses a North American perspective. Adv Virus Res 72:127–154. https://doi.org/10.1016/S0065-3527(08)00403-X.
6. Taubenberger JK, Kash JC. 2010. Influenza virus evolution, host adaptation, and pandemic formation. Cell Host Microbe 7:440–451. https://doi.org/10.1016/j.chom.2010.05.009.
7. Cox NJ, Subbarao K. 2000. Global epidemiology of influenza: past and present. Annu Rev Med 51:407–421. https://doi.org/10.1146/annurev.med.51.1.407.
8. To KK, Ng KH, Que TL, Chan JM, Tsang KY, Tsang AK, Chen H, Yuen KY. 2012. Avian influenza A H5N1 virus: a continuous threat to humans. Emerg Microbes Infect 1:e25. https://doi.org/10.1038/emi.2012.24.
9. Beigel JH, Farrar J, Han AM, Hayden FG, Hyer R, de Jong MD, Lochindarat S, Nguyen TK, Nguyen TH, Tran TH, Nicoll A, Touch S, Yuen KY; Writing Committee of the World Health Organization (WHO) Consultation on Human Influenza A/H5. 2005. Avian influenza A (H5N1) infection in humans. N Engl J Med 353:1374–1385. https://doi.org/10.1056/NEJMra052211.
10. Hatta M, Gao P, Halfmann P, Kawaoka Y. 2001. Molecular basis for high virulence of Hong Kong H5N1 influenza A viruses. Science 293:1840–1842. https://doi.org/10.1126/science.1062882.
11. Chen L-M, Davis CT, Zhou H, Cox NJ, Donis RO. 2008. Genetic compatibility and virulence of reassortants derived from contemporary avian H5N1 and human H3N2 influenza A viruses. PLoS Pathog 4:e1000072. https://doi.org/10.1371/journal.ppat.1000072.
12. Tundup S, Kandasamy M, Perez JT, Mena N, Steel J, Nagy T, Albrecht RA, Manicassamy B. 2017. Endothelial cell tropism is a determinant of H5N1 pathogenesis in mammalian species. PLoS Pathog 13:e1006270. https://doi.org/10.1371/journal.ppat.1006270.
13. Suguitan AL, Jr, Matsuoka Y, Lau YF, Santos CP, Vogel L, Cheng LI, Orandle M, Subbarao K. 2012. The multibasic cleavage site of the hemagglutinin of highly pathogenic A/Vietnam/1203/2004 (H5N1) avian influenza virus acts as a virulence factor in a host-specific manner in mammals. J Virol 86:2706–2714. https://doi.org/10.1128/JVI.05546-11.
14. Schrauwen EJ, Herfst S, Leijten LM, van Run P, Bestebroer TM, Linster M, Bodewes R, Kreijtz JH, Rimmelzwaan GF, Osterhaus AD, Fouchier RA, Kuiken T, van Riel D. 2012. The multibasic cleavage site in H5N1 virus is critical for systemic spread along the olfactory and hematogenous routes in ferrets. J Virol 86:3975–3984. https://doi.org/10.1128/JVI.06828-11.
15. Veits J, Weber S, Stech O, Breithaupt A, Graber M, Gohrbandt S, Bogs J, Hundt J, Teifke JP, Mettenleiter TC, Stech J. 2012. Avian influenza virus hemagglutinins H2, H4, H8, and H14 support a highly pathogenic phenotype. Proc Natl Acad Sci U S A 109:2579–2584. https://doi.org/10.1073/pnas.1109397109.
16. Gabriel G, Czudai-Matwich V, Klenk H-D. 2013. Adaptive mutations in the H5N1 polymerase complex. Virus Res 178:53–62. https://doi.org/10.1016/j.virusres.2013.05.010.
17. Cauldwell AV, Long JS, Moncorge O, Barclay WS. 2014. Viral determinants of influenza A virus host range. J Gen Virol 95:1193–1210. https://doi.org/10.1099/vir.0.062836-0.
18. Steel J, Lowen AC, Mubareka S, Palese P. 2009. Transmission of influenza virus in a mammalian host is increased by PB2 amino acids 627K or 627E/701N. PLoS Pathog 5:e1000252. https://doi.org/10.1371/journal.ppat.1000252.
19. Yamada S, Hatta M, Staker BL, Watanabe S, Imai M, Shinya K, Sakai-Tagawa Y, Ito M, Ozawa M, Watanabe T, Sakabe S, Li C, Kim JH, Myler PJ, Phan I, Raymond A, Smith E, Stacy R, Nidom CA, Lank SM, Wiseman RW, Bimber BN, O'Connor DH, Neumann G, Stewart LJ, Kawaoka Y. 2010. Biological and structural characterization of a host-adapting amino acid in influenza virus. PLoS Pathog 6:e1001034. https://doi.org/10.1371/journal.ppat.1001034.
20. Taft AS, Ozawa M, Fitch A, Depasse JV, Halfmann PJ, Hill-Batorski L, Hatta M, Friedrich TC, Lopes TJ, Maher EA, Ghedin E, Macken CA, Neumann G, Kawaoka Y. 2015. Identification of mammalian-adapting mutations in the polymerase complex of an avian H5N1 influenza virus. Nat Commun 6:7491. https://doi.org/10.1038/ncomms8491.
21. La Gruta NL, Kedzierska K, Stambas J, Doherty PC. 2007. A question of self-preservation: immunopathology in influenza virus infection. Immunol Cell Biol 85:85–92. https://doi.org/10.1038/sj.icb.7100026.
22. Duan S, Thomas PG. 2016. Balancing immune protection and immune pathology by CD8(+) T-cell responses to influenza infection. Front Immunol 7:25. https://doi.org/10.3389/fimmu.2016.00025.
23. Korteweg C, Gu J. 2008. Pathology, molecular biology, and pathogenesis of avian influenza A (H5N1) infection in humans. Am J Pathol 172:1155–1170. https://doi.org/10.2353/ajpath.2008.070791.
24. de Jong MD, Simmons CP, Thanh TT, Hien VM, Smith GJ, Chau TN, Hoang DM, Chau NV, Khanh TH, Dong VC, Qui PT, Cam BV, Ha DQ, Guan Y, Peiris JS, Chinh NT, Hien TT, Farrar J. 2006. Fatal outcome of human influenza A (H5N1) is associated with high viral load and hypercytokinemia. Nat Med 12:1203–1207. https://doi.org/10.1038/nm1477.
25. Ramos I, Bernal-Rubio D, Durham N, Belicha-Villanueva A, Lowen AC, Steel J, Fernandez-Sesma A. 2011. Effects of receptor binding specificity of avian influenza virus on the human innate immune response. J Virol 85:4421–4431. https://doi.org/10.1128/JVI.02356-10.
26. Perrone LA, Plowden JK, Garcia-Sastre A, Katz JM, Tumpey TM. 2008. H5N1 and 1918 pandemic influenza virus infection results in early and excessive infiltration of macrophages and neutrophils in the lungs of mice. PLoS Pathog 4:e1000115. https://doi.org/10.1371/journal.ppat.1000115.
27. Baskin CR, Bielefeldt-Ohmann H, Tumpey TM, Sabourin PJ, Long JP, Garcia-Sastre A, Tolnay AE, Albrecht R, Pyles JA, Olson PH, Aicher LD, Rosenzweig ER, Murali-Krishna K, Clark EA, Kotur MS, Fornek JL, Proll S, Palermo RE, Sabourin CL, Katze MG. 2009. Early and sustained innate immune response defines pathology and death in nonhuman primates infected by highly pathogenic influenza virus. Proc Natl Acad Sci U S A 106:3455–3460. https://doi.org/10.1073/pnas.0813234106.
28. Hatta Y, Hershberger K, Shinya K, Proll SC, Dubielzig RR, Hatta M, Katze MG, Kawaoka Y, Suresh M. 2010. Viral replication rate regulates clinical outcome and CD8 T cell responses during highly pathogenic H5N1 influenza virus infection in mice. PLoS Pathog 6:e1001139. https://doi.org/10.1371/journal.ppat.1001139.
29. Kandasamy M, Suryawanshi A, Tundup S, Perez JT, Schmolke M, Manicassamy S, Manicassamy B. 2016. RIG-I signaling is critical for efficient polyfunctional T cell responses during influenza virus infection. PLoS Pathog 12:e1005754. https://doi.org/10.1371/journal.ppat.1005754.
30. Rutigliano JA, Sharma S, Morris MY, Oguin TH, III, McClaren JL, Doherty PC, Thomas PG. 2014. Highly pathological influenza A virus infection is associated with augmented expression of PD-1 by functionally compromised virus-specific CD8+ T cells. J Virol 88:1636–1651. https://doi.org/10.1128/JVI.02851-13.
31. Sun K, Torres L, Metzger DW. 2010. A detrimental effect of interleukin-10 on protective pulmonary humoral immunity during primary influenza A virus infection. J Virol 84:5007–5014. https://doi.org/10.1128/JVI.02408-09.
32. Valero-Pacheco N, Arriaga-Pizano L, Ferat-Osorio E, Mora-Velandia LM, Pastelin-Palacios R, Villasís-Keever MÁ, Alpuche-Aranda C, Sánchez-Torres LE, Isibasi A, Bonifaz L, López-Macías C. 2013. PD-L1 expression induced by the 2009 pandemic influenza A(H1N1) virus impairs the human T cell response. Clin Dev Immunol 2013:989673. https://doi.org/10.1155/2013/989673.
33. Slutter B, Van Braeckel-Budimir N, Abboud G, Varga SM, Salek-Ardakani S, Harty JT. 2017. Dynamics of influenza-induced lung-resident memory T cells underlie waning heterosubtypic immunity. Sci Immunol 2:eaag2031. https://doi.org/10.1126/sciimmunol.aag2031.
34. Takamura S, Yagi H, Hakata Y, Motozono C, McMaster SR, Masumoto T, Fujisawa M, Chikaishi T, Komeda J, Itoh J, Umemura M, Kyusai A, Tomura M, Nakayama T, Woodland DL, Kohlmeier JE, Miyazawa M. 2016. Specific niches for lung-resident memory CD8+ T cells at the site of tissue regeneration enable CD69-independent maintenance. J Exp Med 213:3057–3073. https://doi.org/10.1084/jem.20160938.
35. Turner DL, Bickham KL, Thome JJ, Kim CY, D'Ovidio F, Wherry EJ, Farber DL. 2014. Lung niches for the generation and maintenance of tissue-resident memory T cells. Mucosal Immunol 7:501–510. https://doi.org/10.1038/mi.2013.67.

36. Mueller SN, Mackay LK. 2016. Tissue-resident memory T cells: local specialists in immune defence. Nat Rev Immunol 16:79–89. https://doi.org/10.1038/nri.2015.3.
37. Peiris JS, Cheung CY, Leung CY, Nicholls JM. 2009. Innate immune responses to influenza A H5N1: friend or foe? Trends Immunol 30:574–584. https://doi.org/10.1016/j.it.2009.09.004.
38. Korteweg C, Gu J. 2010. Pandemic influenza A (H1N1) virus infection and avian influenza A (H5N1) virus infection: a comparative analysis. Biochem Cell Biol 88:575–587. https://doi.org/10.1139/O10-017.
39. Uyeki TM. 2009. Human infection with highly pathogenic avian influenza A (H5N1) virus: review of clinical issues. Clin Infect Dis 49:279–290. https://doi.org/10.1086/600035.
40. Aldridge JR, Jr, Moseley CE, Boltz DA, Negovetich NJ, Reynolds C, Franks J, Brown SA, Doherty PC, Webster RG, Thomas PG. 2009. TNF/iNOS-producing dendritic cells are the necessary evil of lethal influenza virus infection. Proc Natl Acad Sci U S A 106:5306–5311. https://doi.org/10.1073/pnas.0900655106.
41. Yu WC, Chan RW, Wang J, Travanty EA, Nicholls JM, Peiris JS, Mason RJ, Chan MC. 2011. Viral replication and innate host responses in primary human alveolar epithelial cells and alveolar macrophages infected with influenza H5N1 and H1N1 viruses. J Virol 85:6844–6855. https://doi.org/10.1128/JVI.02200-10.
42. Wells MA, Albrecht P, Ennis FA. 1981. Recovery from a viral respiratory infection. I. Influenza pneumonia in normal and T-deficient mice. J Immunol 126:1036–1041.
43. Erickson JJ, Gilchuk P, Hastings AK, Tollefson SJ, Johnson M, Downing MB, Boyd KL, Johnson JE, Kim AS, Joyce S, Williams JV. 2012. Viral acute lower respiratory infections impair CD8+ T cells through PD-1. J Clin Invest 122:2967–2982. https://doi.org/10.1172/JCI62860.
44. Erickson JJ, Rogers MC, Tollefson SJ, Boyd KL, Williams JV. 2016. Multiple inhibitory pathways contribute to lung CD8+ T cell impairment and protect against immunopathology during acute viral respiratory infection. J Immunol 197:233–243. https://doi.org/10.4049/jimmunol.1502115.
45. Yao S, Jiang L, Moser EK, Jewett LB, Wright J, Du J, Zhou B, Davis SD, Krupp NL, Braciale TJ, Sun J. 2015. Control of pathogenic effector T-cell activities in situ by PD-L1 expression on respiratory inflammatory dendritic cells during respiratory syncytial virus infection. Mucosal Immunol 8:746–759. https://doi.org/10.1038/mi.2014.106.
46. Staples KJ, Nicholas B, McKendry RT, Spalluto CM, Wallington JC, Bragg CW, Robinson EC, Martin K, Djukanovic R, Wilkinson TM. 2015. Viral infection of human lung macrophages increases PDL1 expression via IFNbeta. PLoS One 10:e0121527. https://doi.org/10.1371/journal.pone.0121527.
47. Zhu J, Chen H, Huang X, Jiang S, Yang Y. 2016. Ly6Chi monocytes regulate T cell responses in viral hepatitis. JCI Insight 1:e89880. https://doi.org/10.1172/jci.insight.89880.
48. Wu T, Hu Y, Lee YT, Bouchard KR, Benechet A, Khanna K, Cauley LS. 2014. Lung-resident memory CD8 T cells (TRM) are indispensable for optimal cross-protection against pulmonary virus infection. J Leukoc Biol 95:215–224. https://doi.org/10.1189/jlb.0313180.
49. Casey KA, Fraser KA, Schenkel JM, Moran A, Abt MC, Beura LK, Lucas PJ, Artis D, Wherry EJ, Hogquist K, Vezys V, Masopust D. 2012. Antigen-independent differentiation and maintenance of effector-like resident memory T cells in tissues. J Immunol 188:4866–4875. https://doi.org/10.4049/jimmunol.1200402.
50. Mackay LK, Rahimpour A, Ma JZ, Collins N, Stock AT, Hafon ML, Vega-Ramos J, Lauzurica P, Mueller SN, Stefanovic T, Tscharke DC, Heath WR, Inouye M, Carbone FR, Gebhardt T. 2013. The developmental pathway for CD103(+)CD8+ tissue-resident memory T cells of skin. Nat Immunol 14:1294–1301. https://doi.org/10.1038/ni.2744.
51. Zhang N, Bevan MJ. 2013. Transforming growth factor-beta signaling controls the formation and maintenance of gut-resident memory T cells by regulating migration and retention. Immunity 39:687–696. https://doi.org/10.1016/j.immuni.2013.08.019.
52. Carlson CM, Turpin EA, Moser LA, O'Brien KB, Cline TD, Jones JC, Tumpey TM, Katz JM, Kelley LA, Gauldie J, Schultz-Cherry S. 2010. Transforming growth factor-beta: activation by neuraminidase and role in highly pathogenic H5N1 influenza pathogenesis. PLoS Pathog 6:e1001136. https://doi.org/10.1371/journal.ppat.1001136.
53. Schultz-Cherry S, Hinshaw VS. 1996. Influenza virus neuraminidase activates latent transforming growth factor beta. J Virol 70:8624–8629. https://doi.org/10.1128/JVI.70.12.8624-8629.1996.
54. Bergsbaken T, Bevan MJ, Fink PJ. 2017. Local inflammatory cues regulate differentiation and persistence of CD8+ tissue-resident memory T cells. Cell Rep 19:114–124. https://doi.org/10.1016/j.celrep.2017.03.031.
55. Manicassamy B, Manicassamy S, Belicha-Villanueva A, Pisanelli G, Pulendran B, García-Sastre A. 2010. Analysis of in vivo dynamics of influenza virus infection in mice using a GFP reporter virus. Proc Natl Acad Sci U S A 107:11531–11536. https://doi.org/10.1073/pnas.0914994107.
56. Steel J, Lowen AC, Pena L, Angel M, Solorzano A, Albrecht R, Perez DR, Garcia-Sastre A, Palese P. 2009. Live attenuated influenza viruses containing NS1 truncations as vaccine candidates against H5N1 highly pathogenic avian influenza. J Virol 83:1742–1753. https://doi.org/10.1128/JVI.01920-08.
57. Lutz MB, Kukutsch N, Ogilvie AL, Rossner S, Koch F, Romani N, Schuler G. 1999. An advanced culture method for generating large quantities of highly pure dendritic cells from mouse bone marrow. J Immunol Methods 223:77–92. https://doi.org/10.1016/s0022-1759(98)00204-x.
58. Sun J, Madan R, Karp CL, Braciale TJ. 2009. Effector T cells control lung inflammation during acute influenza virus infection by producing IL-10. Nat Med 15:277–284. https://doi.org/10.1038/nm.1929.